derived by the progressive truncation of the vertices of either extreme. Whilst statement (I) is generally true, statement (II) is valid only in special cases.

The observations on the etching of single crystal germanium spheres by Ellis (1954, 1957) and by Batterman (1957) are of interest since they succeeded in producing a number of different geometrical dissolution shapes, including the rhombic dodecahedron. Heimann (1975) shows a photograph of five such shapes; {110}, {*hk*0}, {100}, {*hhl*}, and {111}, all formed by the dissolution of germanium spheres in various acid mixtures. He also gives numerous other examples, lists nearly seven hundred references and reviews the theories of dissolution, notably those of F. C. Frank.

Contrary to earlier beliefs (particularly Goldschmidt and Wright, 1904) that after considerable etching the dissolution body would assume a definite shape (Endkörper), Frank's kinematic theory (1958, 1972) suggests that there is no unique terminal morphology independent of the starting shape. In general, the shape gradually changes throughout the dissolution process.

REFERENCES

Bagdasarov, H. S., Berezhkova, G. V., Govorkov, V. G., and Smirnov, A. E. (1974) *J. Crystal Growth*, **22**, 61–4.

Batterman, B. W. (1957) *J. Appl. Phys.*, **28**, 1236–41.

Bovenkerk, H. P. (1961) *Am. Mineral.*, **46**, 952–63.

——Bundy, F. P., Hall, H. T., Strong, H. M., and Wentorf, R. H. Jr. (1959) *Nature*, **184**, 1094–8.

Donaldson, C. H. (1985) *Mineral. Mag.*, **49**, 129–32.

Ellis, R. C. Jr. (1954) *J. Appl. Phys.*, **25**, 1497–9.

——(1957) Ibid. **28**, 1068.

Frank, F. C. (1958) In *Growth and Perfection of Crystals* (R. H. Doremus, B. W. Roberts, and D. Turnbull, eds.). John Wiley, New York, 411–19.

——(1972) *Z. Physik, Chem., Neue Folge*, **77**, 84–92.

Goldschmidt, V., and Wright, F. E. (1904) *Neues Jahrb. Mineral. Geol. Paläont., Beil.-Bd.* **18**, 335–76.

Heimann, R. B. (1975) *Auflösung von Kristallen*. Springer-Verlag, Wien and New York. xiv + 270 pp.

Litvin, Yu. A., and Butuzov, V. P. (1969) *Soviet Physics—Doklady*, **13**, 746–7.

Moore, M. (1973) *Dissolution, Defects and Disorder in Diamond and Diamond-like Substances*, Vol. I, Ph.D. thesis, University of Bristol, 11–13.

——(1979) In *The Properties of Diamond* (J. E. Field, ed.). Academic Press, London, New York, and San Francisco, 245–77.

——(1985) *Industrial Diamond Review*, **45**, 67–71.

——and Lang, A. R. (1974) *J. Crystal Growth*, **26**, 133–9.

Strong, H. M., and Wentorf, R. H. Jr. (1972) *Naturwiss.* **59**, 1–7.

[*Manuscript received 5 July 1985*]

KEYWORDS: crystal growth, dissolution, morphology.

Department of Physics, Royal Holloway College, University of London, Egham, Surrey, TW20 0EX

MORETON MOORE

MINERALOGICAL MAGAZINE, JUNE 1986, VOL. 50, PP. 332–6

Variations in a growth form of synthetic vaterite

VATERITE, a polymorph of $CaCO_3$, is rarely found in nature but has been identified in the repair tissue of young gastropods (Mayer and Weineck, 1932), in gallstones (Phemister *et al.*, 1939; Rodgers, 1983), in the early carbonation of Portland cements (Cole and Kroone, 1959), in a carbonated hydrogel (McConnell, 1960) and in evaporite beds in the Antarctic (Browne, 1973). Its scarcity in nature compared with the other two polymophs, calcite and aragonite, may be due to its instability in the presence of water. Hitherto, morphological description of vaterite has not been possible because the available material, both natural and synthetic, has been restricted to very small crystals (1–10 μm).

Previously, vaterite has been synthesized at room temperature by precipitation from a solution containing a calcium salt (e.g. Gibson *et al.*, 1925). In our work, which involved a series of experiments to study the distribution of selected trace elements between synthetic $CaCO_3$ and its parent solution, spheroids of vaterite (0.1–1.0 mm diameter) were observed amongst the crystalline products. The syntheses were made by the slow diffusion of CO_2

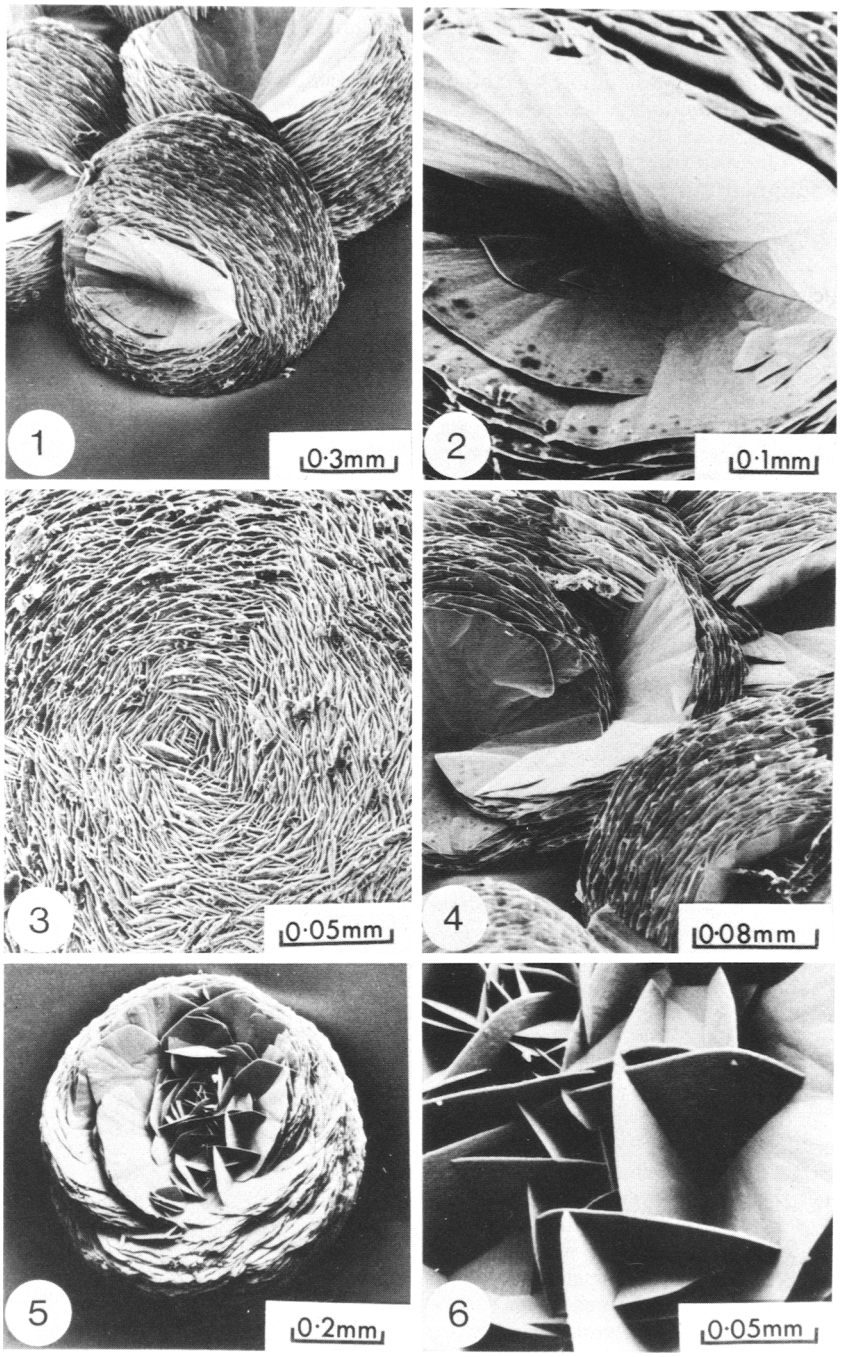

FIGS. 1–6. Scanning electron micrographs of synthetic vaterite. FIG. 1. Incomplete spheroids consisting of joined interleaved sheets. FIG. 2. New fan-shaped sheets which have nucleated in crenellations on previously formed sheets. FIG. 3. Completed spheroid consisting of progressively inclined sheets. FIG. 4. Groups of sheets in approximately perpendicular alignment. FIG. 5. Spheroid completed by near-perpendicular sheets. FIG. 6. Enlarged view of terminal sheets in fig. 5.

(for 3–4 weeks) into a solution containing $CaCl_2$ and NH_4Cl at 20 °C, after the method described by Gruzenski (1967). This method, which allows slow growth of the crystalline materials, was chosen to ensure equilibrium conditions between crystals and parent solution. When the concentration of Co in the parent solution exceeds 50 ppm, all three polymorphs form and are readily distinguishable as pink vaterite spheroids, pink calcite rhombohedra and white aragonite spheroids, the colour difference being a result of the greater partition of Co into calcite and vaterite relative to aragonite (20:20:1).

Three variations of a growth form of vaterite have been identified and are described.

Experimental procedure. 800 ml of base solution containing $CaCl_2$ (0.18 M) and NH_4Cl (3.7 M) and the required concentration of dopant (> 50 ppm Co) added as chloride, were placed in a litre beaker. A vented vial containing 3–4 g of crushed ammonium carbonate ($NH_4HCO_3 \cdot NH_2COONH_4$) was suspended over the solution. A watch glass was placed on the beaker and the assembly was then sealed with a thin plastic film. The beaker was allowed to stand undisturbed for 3–4 weeks at 20 °C, during which time 0.5–1.0 g of $CaCO_3$ crystallized. Vaterite spheroids nucleated and grew on the surface of the beaker, on the edge of calcite rhombohedra and occasionally at the surface of the solution.

The solution was decanted and the crystals rinsed six times with water followed by the same number of washes with alcohol before drying under an infra-red lamp. The hand-separated spheroids were identified as vaterite by X-ray powder diffraction and they were examined using an ISI 60A scanning electron microscope (figs. 1–6). A high resolution examination (figs. 7–10) was also carried out using a Hitachi S800 scanning electron microscope.

Growth forms. Three variations of a growth form of synthetic vaterite were observed, all of which originated as joined interleaved sheets, approximately 2 μm thick (fig. 1).

In one variation, new fan-shaped sheets start on crenellations in previously formed sheets, and grow at a low angle (5–10°) to each other (fig. 2), forming a sheaf of inter-connected sheets in which each successive sheet is more steeply inclined than the previous sheet. A spheroid is formed by the successive growth of these sheets and terminates with a set of small sheets mutually inclined at high angles as shown at the centre of fig. 3.

A second variation consists of groups of subparallel sheets arranged approximately perpendicularly to each other (fig. 4).

The third variation differs from the others in that the development of a spheroid has been changed by the growth of single sheets at high angles to the subparallel sheets formed in the early stages of growth (fig. 5). Unlike the sheets forming the bulk of the spheroid, each of these upstanding sheets has relatively flat surfaces and makes sharp intersections with the others (fig. 6).

High resolution and magnification (20 000 times) (fig. 7) show the surfaces of individual vaterite sheets to be highly irregular with many voids, contrasting with the more regular nature of the broken surfaces of a calcite rhombohedron (fig. 8) and with the growth surfaces of individual aragonite crystals present in a spheroid (fig. 9).

Two spheroids, one of vaterite and the other of aragonite, nucleated separately, grew towards each other and coalesced. The two are joined by slender outgrowths at the points of contact (fig. 10). Vaterite and aragonite have some similarities in their crystal structures: the projection of the average structure of disordered vaterite down the *a*-axis (Kamhi, 1963; Meyer, 1969) closely resembles the asymmetric unit of aragonite projected down the *c*-axis. In contrast, the structure of calcite differs appreciably from that of vaterite and no continuity of growth has been observed between vaterite spheroids and calcite rhombohedra.

It is hoped that the recognition of various growth forms of synthetic vaterite may lead to further identifications of this rare polymorph of $CaCO_3$ in natural materials.

Acknowledgements. The authors would like to thank Drs P. Henderson and J. E. Chisholm for their assistance in the preparation of this manuscript.

REFERENCES

Browne, P. R. L. (1973) Secondary minerals in cores from Dry Valley Drilling Project 1 and 2. *D.V.D.P. Bull.* No. 2, 83–93.

Cole, W. F., and Kroone, B. (1959) Carbonate minerals in hydrated portland cement. *Nature*, Brit. Assoc. Vol. BA, 57.

Gibson, R. E., Wyckoff, R. W. R., and Merwin, H. E. (1925) Vaterite and μ calcium carbonate. *Amer. J. Sci.* 5th Series **10,** 325–33.

Gruzenski, P. M. (1967) Growth of calcite crystals. *J. Phys. Chem. Solids G.B.* Suppl. **1,** 365–7.

Kamhi, S. R. (1963) On the structure of vaterite, $CaCO_3$. *Acta Crystallogr.* **16,** 770–2.

McConnell, J. D. C. (1960) Vaterite from Ballyeraigy, Larne, Northern Ireland. *Mineral. Mag.* **32,** 535–44.

Mayer, F. K., and Weineck, E. (1932) Die Verbreitung des Kalziumkarbonates im Tierreich unter besonderer Berücksichtigung der Wirbellosen. *Jena Z. Naturw.* **66,** 199–222.

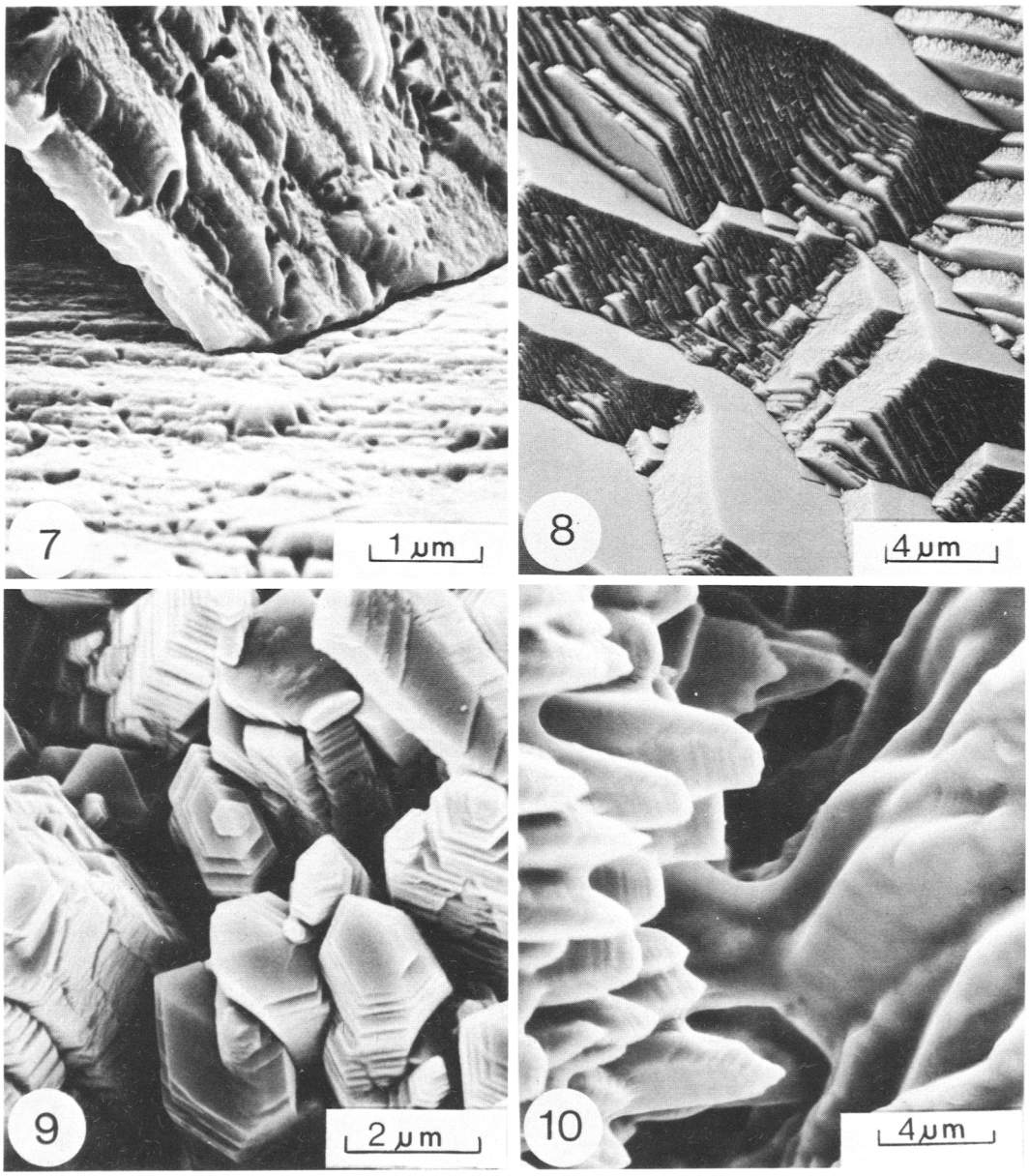

FIGS. 7–10. High-magnification scanning electron micrographs. FIG. 7. Intersection of two sheets of vaterite showing the porous nature of the growth surfaces. FIG. 8. Broken surface of a calcite crystal showing its compact nature. FIG. 9. Growth surfaces of aragonite crystals present in a spheroid, which also show a relatively compact nature in comparison with that of vaterite sheets. FIG. 10. Contact between independently nucleated spheroids of aragonite (left) and vaterite (right).

Meyer, H. J. (1969) Struktur und Fehlordnung des Vaterits. *Z. Kristallogr.* **128,** 183 212.
Phemister, D. B., Aounsohn, M. G., and Pepensky, R. (1939) Variations in the cholesterol bile pigment and calcium salts contents of gallstones formed in gallbladder and in bile ducts with the degree of associated obstruction. *Ann. Surg.* **109,** 161-86.
Rodgers, A. L. (1983) Common ultrastructural features in human calculi. *Micron Microscopia Acta,* **14,** 219-24.

[*Manuscript received 14 October 1985; revised 15 January 1986*]

KEYWORDS: vaterite, crystal growth, carbonates.

Department of Mineralogy,
Department of Central Services, British Museum (Natural History),
Cromwell Road, London SW7 5BD

A. J. EASTON
D. CLAUGHER

MINERALOGICAL MAGAZINE, JUNE 1986, VOL. 50, PP. 336 40

Some observations on the chemical composition of todorokite

TODOROKITE is one of the major manganese oxide minerals in marine ferromanganese nodules occurring on the ocean floor, and it also occurs in significant amounts in terrestrial manganese deposits, in weathering zones and in soils. Discovered fifty years ago in Japan as a weathering product of inesite, $Ca_2Mn_7Si_{10}O_{28}(OH)_2 \cdot 5H_2O$ (Yoshimura, 1934), its structure and chemical composition are still matters of debate. Uncertainties as to structure arose chiefly because its X-ray powder diffraction pattern was somewhat similar to that of a sodium manganese manganate hydrate synthesized by Wadsley (1950) and because this pattern was also similar to one of the patterns observed in marine ferromanganese nodules by Buser and Grutter (1956). The phase producing this particular pattern was named by Buser (1959), 10 Å manganite. The controversy over the nature of these marine, terrestrial, and synthetic phases has produced an abundant literature (Burns and Burns, 1977, 1979) but little consensus of opinion. Agreement has however been reached over the status of todorokite (Giovanoli, 1985; Burns *et al.*, 1985).

During the last decade electron microscopy (EM), both scanning (SEM) and high resolution transmission (HRTEM), has been increasingly used in the study of these phases. At optical magnifications, terrestrial todorokite appears as prismatic crystals or as masses of parallel fibres (Chukhrov *et al.*, 1978, 1980). Under the SEM marine todorokite has been identified as fibrous masses (Burns and Burns, 1978) and as platelets (Lallier-Verges and Clinard, 1983). The use of HRTEM has given abundant evidence that the plate morphology is really the result of sheets of fibres (Giovanoli, 1980) which at high magnification show dark and light bands interpreted as manganese oxide tunnels (Turner and Buseck, 1981). A characteristic feature of these sheets is the presence of twinning at 120° (trillings). The basic tunnel width of todorokite is three $[Mn^{4+}O_6]$ octahedral chains, or about 9.6 Å (Siegel and Turner, 1982), but natural todorokites contain a variety of tunnel dimensions (Turner *et al.*, 1982). At the present time the term todorokite is widely accepted for the complex tunnel structure in both marine and terrestrial deposits which give an X-ray diffraction pattern with major lines at, or close to, 9.6, 4.8, 2.4, and 1.4 Å (Burns and Burns, 1977). Whether this tunnel structure is the *only* phase in marine nodules giving an X-ray pattern similar to the above is still under investigation (Chukhrov *et al.*, 1983).

This paper is not directed at the question of todorokite crystal structure but at its chemical composition. This is known to be complex and variable (Burns and Burns, 1977). A number of approximate formulae exist. That of Frondel *et al.* (1960), $(Ca,Na,K,Ba,Ag)(Mg,Mn^{2+},Zn)Mn_5^{4+}O_{12} \cdot xH_2O$ is widely used. The most recent paper on todorokite (Burns *et al.*, 1983) indicates that the large cations Ca^{2+}, Ba^{2+}, Na^+, and K^+ occupy the tunnels between the $[Mn^{4+}O_6]$ chains while ions such as Mg^{2+} and Zn^{2+} substitute for Mn^{2+} in the